The $B_1 \rightleftharpoons B_2$ phase transition in alkaline-earth oxides: a comparison of *ab initio* Hartree-Fock and density functional calculations

1998 J. Phys.: Condens. Matter 10 6897

(http://iopscience.iop.org/0953-8984/10/31/008)

J. Phys.: Condens. Matter **10** (1998) 6897–6909. Printed in the UK PII: S0953-8984(98)92050-1

The $B_1 \rightleftharpoons B_2$ phase transition in alkaline-earth oxides: a comparison of *ab initio* Hartree–Fock and density functional calculations

Marie-Pierre Habas†, Roberto Dovesi‡ and Albert Lichanot†

† Laboratoire de Chimie Structurale, UMR 5624, IFR rue Jules Ferry, 64000 Pau, France

‡ Department CIFM, University of Torino, via Giuria 5, I-10125 Torino, Italy

Received 26 February 1998

Abstract. Structural properties of the B_1 (NaCl-type) and B_2 (CsCl-type) phases of alkaline-earth oxides and their phase transition have been investigated with the periodic *ab initio* linear combination of atomic orbitals method implemented in the CRYSTAL program. The geometries have been optimized and the bulk modulus evaluated. The calculations have been done at the Hartree–Fock (HF) and density functional theory (DFT) levels. In this last case, the exchange–correlation potential correcting the electronic density uses either one local or three non-local models. The comparison of the different approaches allows us to identify a trend, in order to obtain results in better agreement with experiment.

1. Introduction

Because the alkaline-earth oxides MgO, CaO, SrO and BaO are important constituents of the Earth's lower mantle, where the pressure reaches 140 GPa, several experimental and theoretical studies have been carried out with the aim of formulating a description of their high-pressure behaviour. A few experimental studies of the phase transitions occurring in these oxides have been realized [1–8]. The phase transition from B_1 (NaCl-type) to B_2 (CsCl-type) phases has been observed experimentally at pressures of 60 [3], 65 [4] and 63 [5] (CaO), 36 [6] (SrO) and 9 [7] and 14.5 [8] (BaO) GPa. For MgO, the $B_1 \rightleftharpoons B_2$ phase transition has been observed up to 120 GPa [1, 2] and this illustrates the experimental difficulties encountered in the study of phases under very high pressures. The use of theoretical methods is therefore justified in order to obtain information about the structures of materials at high pressures.

Many calculations using different approaches have been carried out separately for each compound. Generally speaking, it is difficult to obtain consistent results in satisfactory agreement with experiment, particularly for MgO [9–12].

In the present paper, the structural and mechanical properties of the B_1 and B_2 phases of the four compounds are investigated and the $B_1 \rightleftharpoons B_2$ transition volumes and pressures are deduced by considering the Murnaghan equation of state [13]. To do this, the linear combination of atomic orbitals (LCAO) self-consistent-field (SCF) method implemented in the CRYSTAL program [14] is used. The light elements (Mg, Ca and O) are described with all-electron basis sets whereas an effective-core pseudopotential (ECP) is adopted to describe heavier elements. Thanks to the CRYSTAL95 [14] code, the calculations can be done at both the Hartree–Fock and density functional levels. In this latter approach, the

0953-8984/98/316897+13$19.50

correction of the electronic density is considered—using exchange–correlation potentials parametrized according to one local (local density approximation: LDA) and different non-local (generalized gradient approximation: GGA) models. Comparison of these theoretical results with the available experimental data should enable us to select the best method(s) for describing the structural and mechanical properties of simple closed-shell systems satisfactorily.

2. Computational details

2.1. The ab initio program

For the present calculations, the CRYSTAL95 computer program [14] was used. We refer the reader to previous papers [15, 16] for a description of the periodic LCAO self-consistent-field computational scheme as implemented in such a code. The CRYSTAL95 code contains a density functional theory (DFT) option that permits one to solve the Kohn–Sham (KS) equations self-consistently. The exchange–correlation (XC) potential is expanded in an auxiliary basis set of symmetrized atom-centred Gaussian-type functions (GTFs). In this work, one local and three non-local exchange–correlation potentials have been used; they will be indicated as follows: LP for LDA [17] (exchange) and PZ [18] (correlation); BL for B [19] (exchange) and LYP [20] (correlation); PBE [21] (exchange and correlation); PP [22] (exchange and correlation). Good computational conditions for the evaluation of the Coulomb and exchange series as defined in references [15, 16] have been used, ensuring high numerical accuracy. As regards the reciprocal-space net, a shrinking factor $S = 8$ has been used, corresponding to 29 and 35 $\boldsymbol{k}$-points for the B_1 and B_2 phases, respectively.

2.2. Basis sets

As regards the basis set, Bloch functions are constructed from local functions (atomic orbitals) which, in turn, are linear combinations (contractions) of GTFs each expressed as the product of a Gaussian and a real solid spherical harmonic. For light atoms (Mg, Ca and O), all-electron (AE) basis sets have been used, whereas for Sr and Ba, the Hay–Wadt small-core ECPs [23] have been adopted. In order to check the quality of the ECPs adopted and their influence on the results, the calculations for CaO have been repeated at the ECP level. The oxygen basis set can be denoted as an 8-411-(1d)G contraction (the first shell is of s type and is a contraction of eight GTFs, then there are three sp shells and one d shell): this notation is similar to that used in a previous study on Cr_2O_3 [24] and for many other oxides. The Mg and Ca (AE) basis sets are 8-511-(1d)G and 8-6511-(3d)G contractions, respectively, and have been used in previous studies of MgO [25] and CaF_2 [26], respectively. The ECP basis set for Ca, Sr and Ba is a 3-1(1d)G contraction (in this case both shells are of sp type).

The exponents of the most diffuse sp and d shells of each atom have been optimized by searching for the minimum Hartree–Fock crystalline total energy. The results obtained are given in table 1. The same basis set has been used for the calculations performed with the various DFT schemes.

Table 1 gives the optimized exponents of the two most diffuse sp ($\alpha_{sp}^{(n-1)}$ and $\alpha_{sp}^{(n)}$) and d shells of each element. Generally speaking, the exponent of a given GTF of alkaline-earth and oxygen elements does not differ significantly in phases B_1 and B_2 except for Mg (the last sp and d shells) and Ca (the d shell) when described with an ECP. This result shows that the basis set for the four oxides which have a fully ionic character in the B_1

Table 1. The exponents (Bohr^{-2}) of the most diffuse Gaussian-type functions (GTFs) of the AO basis sets adopted in the present study. MgO and CaO (AE) are described with all-electron (AE) basis sets whereas the Hay–Wadt small-core pseudopotential was used for Ca (PS), Sr and Ba. The d shell of the Ca AE basis set is described by a contraction of three GTFs whose coefficients are given in parentheses.

	Oxides		$\alpha_{sp}^{(n-1)}$	$\alpha_{sp}^{(n)}$	α_d	
MgO	B_1	Mg	0.689	0.345	0.657	
	B_2		0.683	0.280	0.611	
	B_1	O	0.475	0.183	0.600	
	B_2		0.480	0.184	0.600	
CaO (AE)	B_1	Ca	0.470	0.255		
					3.922	(0.139)
					1.095	(0.326)
					0.380	(0.427)
	B_2		0.475	0.260		
	B_1	O	0.473	0.166	0.600	
	B_2		0.480	0.165	0.600	
CaO (PS)	B_1	Ca	—	0.500	0.620	
	B_2		—	0.495	0.670	
	B_1	O	0.435	0.145	0.600	
	B_2		0.450	0.155	0.600	
SrO	B_1	Sr	—	0.256	0.504	
	B_2		—	0.258	0.516	
	B_1	O	0.488	0.163	0.600	
	B_2		0.486	0.157	0.600	
BaO	B_1	Ba	—	0.213	0.330	
	B_2		—	0.212	0.330	
	B_1	O	0.478	0.155	0.600	
	B_2		0.491	0.166	0.600	

and B_2 phases does not depend on the surroundings of each ion (six and eight nearest neighbours in the B_1 and B_2 phases, respectively) but is rather sensitive to the ratio of the cation (M^{2+}) and O^{2-} sizes, as illustrated by the ratio of the square root of the spheropole $QR(M^{2+})/QR(O^{2-})$ which has different values for the B_1 and B_2 phases only for MgO (see table 6, later). The exponents of the two most diffuse oxygen sp shells are similar for all of the compounds. To compare the results obtained with the use of ECP and AE basis sets, CaO was studied using the two sets. In the case where Ca is described using the Hay–Wadt small-core pseudopotential, the 3d shell has been represented by a contraction either of one GTF (table 1) or of three GTFs (as for the AE set) with the following optimized exponents: $\alpha_d^{(1)} = 3.713$, $\alpha_d^{(2)} = 1.036$ and $\alpha_d^{(3)} = 0.359$, and the same coefficients as for the AE basis set. For reasons of clarity and of homogeneity with SrO and BaO, the results obtained with the use of this last set are not reported in the following because they are not significantly different from those obtained with the d shell described with a unique GTF. For example, the lattice parameter and the bulk modulus of phase B_1 calculated at the HF level are 4.84 Å

Table 2. Equilibrium lattice parameters (Å) calculated at the HF and different DFT levels. Differences (%) with respect to the experiment[a] are given in parentheses for the B_1 phase. Results of others' calculations and experimental data are given for comparison. The DFT notation corresponds to the exchange–correlation potentials used in the local and non-local approximations: LP: LDA/Perdew–Zunger(PZ); BL: Becke/Lee–Yang–Parr; PBE: Perdew–Burke–Ernzerhof/Perdew–Burke–Ernzerhof; PP: Perdew–Wang/Perdew–Wang.

		HF	LP	BL	PBE	PP	Exper-iment	Other calculations		
MgO	B_1	4.20 (0.0)	4.16 (−1.0)	4.27 (+1.7)	4.24 (+1.0)	4.24 (+1.0)	4.20[a] 4.21[d]	—	4.21[b]	4.30[c]
	B_2	2.60	2.60	2.67	2.65	2.65		—	—	—
CaO (AE)	B_1	4.86 (+1.0)	4.71 (−2.0)	4.87 (+1.2)	4.83 (+0.4)	4.82 (+0.2)	4.81[a] 4.81[d,e,f]	—	4.71[b]	4.82[c]
	B_2	2.95	2.86	2.97	2.94	2.93		—	—	—
CaO (PS)	B_1	4.87 (+1.2)	4.75 (−1.2)	4.89 (+1.7)	4.86 (+1.0)	4.85 (+0.8)	4.81[a] 4.81[d,e,f]	—	4.71[b]	4.82[c]
	B_2	2.95	2.87	2.97	2.94	2.94		—	—	—
SrO	B_1	5.22 (+1.2)	5.06 (−1.9)	—	—	—	5.16[a] 5.16[d,h]	5.23[g]	5.06[b]	5.13[c]
	B_2	3.14	3.04	—	—	—		—	—	—
BaO	B_1	5.65 (+2.4)	5.46 (−1.1)	—	—	—	5.52[a] 5.54[d]	—	—	5.49[c]
	B_2	3.39	3.27	—	—	—		—	—	—

[a] Reference [33].
[b] Reference [9].
[c] Reference [10].
[d] Reference [34].
[e] Reference [3].
[f] Reference [35].
[g] Reference [27].
[h] Reference [36].

and 124 GPa, respectively and compare favourably with the values of 4.87 Å (table 2) and 121 GPa (table 4—see later) obtained with a unique GTF for the Ca d shell. CaO is however less stable by 8.6 mHartree with this last set.

2.3. The $B_1 \rightleftharpoons B_2$ transition

The total energies of the four systems in the B_1 and B_2 phases has been evaluated at 25 different volumes, and fitted with the Murnaghan [13] equation of state:

$$E(V) = BV_0\left[\frac{1}{B'(B'-1)}\left(\frac{V_0}{V}\right)^{B'-1} + \frac{1}{B'}\frac{V}{V_0} - \frac{1}{B'-1}\right] + E_0 \qquad (1)$$

where E_0, V_0, B and B' are the equilibrium energy, the equilibrium volume, and the bulk modulus and its pressure derivative. The pressure versus volume relationship is easily obtained by differentiation of the above equation.

Table 3. Binding energies (au) expressed with respect to the atomic references. Differences (%) with respect to the experiment[a] are given in parentheses for the B_1 phase. The symbols HF, LP, BL, B, PBE, PP are defined in table 2: P91 indicates Perdew and Wang (1991) [32].

		HF	LP	BL	HF + PZ	HF + B	HF + PBE	HF + PP	HF + P91	Exper-iment[a]
MgO	B_1	0.276	0.435	0.351	0.338	0.370	0.357	0.357	0.360	0.38
		(−27.4)	(+13.1)	(−7.9)	(−11.0)	(−2.6)	(−6.0)	(−6.0)	(−5.3)	
	B_2	0.208	0.380	0.292	0.270	0.306	0.293	0.293	0.296	—
CaO (AE)	B_1	0.281	0.466	0.381	0.348	0.375	0.364	0.364	0.367	0.40
		(−30.0)	(+16.5)	(−4.7)	(−12.5)	(−6.2)	(−9.0)	(−9.0)	(−8.2)	
	B_2	0.238	0.434	0.343	0.306	0.341	0.327	0.327	0.330	—
SrO	B_1	0.255	—	—	0.321	0.353	0.336	0.337	0.339	0.38
		(−32.9)	—	—	(−15.5)	(−7.1)	(−11.6)	(−11.3)	(−10.8)	
	B_2	0.219	—	—	0.287	0.322	0.308	0.308	0.311	—
BaO	B_1	0.224	—	—	0.289	0.315	0.306	0.306	0.309	0.37
		(−39.4)	—	—	(−21.9)	(−14.9)	(−17.3)	(−17.3)	(−16.5)	
	B_2	0.193	—	—	0.259	0.297	0.283	0.283	0.286	—

[a] Deduced from the *Janaf Thermodynamical Tables* (reference [37]).

As we are working at $T = 0$ K, the transition pressure corresponds to the point where the enthalpy

$$H(p) = E_0 + pV = E_0 + \frac{BV_0}{B' - 1}\left[\left(\frac{B'}{B}p + 1\right)^{1-1/B'} - 1\right] \tag{2}$$

of the B_2 phase is equal to the corresponding quantity for the B_1 phase.

3. Results and discussion

3.1. Geometry and binding energy

The equilibrium lattice parameters and binding energies of the B_1 and B_2 phases of the four compounds are compared in tables 2 and 3 with the results of previous calculations and experimental data. At the HF level, the B_1 lattice parameters are overestimated, as expected, with respect to experiment. The difference ranges from zero (MgO) to 2.4% (BaO) as a consequence of the increasing relative importance of the electron correlation effects (disregarded at the HF level) as the cation becomes larger and the electrostatic forces less important. Also the gradient-corrected DFT schemes (BL, PBE, PP) overestimate the lattice parameters (although to a lesser extent than at the HF level), whereas at the LDA level the underestimation is about equivalent to, or even larger than the HF overestimation. The trend is similar for the B_1 and B_2 phases.

The agreement between our HF results and that obtained by Zupan *et al* [27] for SrO is not surprising because the same computational method and computer program were used. The LDA results reported by Kalpana *et al* [9] (obtained with the tight-binding linear muffin-tin orbital method) are also in reasonable agreement with the present ones (with the LP functional), whereas in the case of the results of Mehl *et al* [10], a larger discrepancy is observed, in particular for MgO and CaO. In the latter case, however, the potential-induced breathing model (PIBM) method has been used, which is an improved version of

Table 4. Equilibrium parameters obtained with the equation of state of Murnaghan at the Hartree–Fock and density functional theory levels. V_0, B and B' are the equilibrium volume (Å^3), the bulk modulus (GPa) and the derivative dB/dp, respectively. The symbols LP, BL, PBE and PP are defined in table 2.

			B_1			B_2		
			V_0	B	B'	V_0	B	B'
MgO	This work	HF	18.4	182	3.92	17.6	181	4.00
		LP	18.0	181	3.70	17.6	170	3.66
		BL	19.5	153	3.66	19.0	147	3.50
		PBE	19.1	160	3.69	18.7	153	3.48
		PP	19.1	159	3.74	18.6	155	3.47
	Experiment		—	162.0[a]	—	—	—	—
			18.5[b]	—	—	—	—	—
	Other calculations		18.7[c]	167.6[c]	—	17.6[c]	—	—
			18.1[d]	172.0[d]	—	—	—	—
			18.4[e]	146.0[e]	—	18.1[e]	—	—
CaO (AE)	This work	HF	28.7	120	4.44	25.6	122	4.05
		LP	26.2	135	3.97	23.3	136	4.30
		BL	28.9	111	3.67	26.2	107	3.79
		PBE	28.2	114	3.91	25.4	114	3.68
		PP	28.0	116	3.82	25.2	113	4.25
	Experiment		27.8[f]	111.2[f]	4.9[f]	—	—	—
			27.8[g]	111.2[g]	4.2[g]	24.6[g]	130.0[g]	3.5[g]
			—	112.0[h]	—	24.7[h]	115.0[h]	4.9[h]
			27.8[i]	115.0[i]	—	24.7[i]	115.0[i]	4.9[i]
	Other calculations		26.1[c]	133.8[c]	—	22.8[c]	—	—
			26.2[d]	129.0[d]	—	—	—	—
			28.0[j]	109.0[j]	4.60[j]	24.0[j]	123.0[j]	4.40[j]

the semi-empirical Gordon–Kim model [28–30] where the short-range pair interactions are parametrized.

The binding energy BE is calculated as the difference between the bulk equilibrium energy and the atomic energies. These latter have been obtained by adding to the basis set of table 1 one sp shell and reoptimizing the exponents of the three most diffuse shells. The same scheme has been adopted for oxygen. The BE values have been calculated according to two methods in order to analyse separately the effect of the exchange and correlation energies. In the first method, the same approaches (HF, LP and BL) are used to calculate the bulk and atomic energies. These latter are obtained thanks to the GAUSSIAN94 [31] code for the compounds described in AE basis sets. In the second method an '*a posteriori*' correlation correction to the HF bulk and atomic energies has been included. It is based on the correlation-only functional of either Perdew and Zunger (PZ), in the local approximation, or Becke (B), Perdew, Burke and Ernzerhof (PBE) and Perdew and Wang (1991) [32] (P91), in the generalized gradient approximation, and the corresponding results are reported in the columns headed HF + PZ, HF + B, HF + PBE and HF + P91 of table 3, respectively. In all cases the BE of the B_1 phase is greater than that of the B_2 phase indicating that B_1 is the most stable phase at $p = 0$. Generally speaking, the theoretical binding energies

Table 4. (Continued)

			B_1			B_2		
			V_0	B	B'	V_0	B	B'
CaO (PS)	This work	HF	28.9	121	4.09	25.6	132	3.95
		LP	26.8	138	4.06	23.6	153	3.89
		BL	29.3	114	3.75	26.1	128	3.54
		PBE	28.7	117	3.72	25.5	128	3.73
		PP	28.6	117	3.81	25.4	129	3.74
SrO	This work	HF	35.5	101	4.12	31.1	107	4.08
		LP	32.3	124	4.05	28.1	130	4.12
	Experiment		34.3[k]	—	—	—	—	—
			—	91.3[h,i]	—	—	—	—
			—	90.6[l]	—	—	—	—
	Other calculation		32.4[c]	109.8[c]	—	—	—	—
BaO	This work	HF	45.0	81	4.21	38.9	92	4.07
		LP	40.8	100	4.64	34.9	117	4.29
	Experiment		—	72.2[f]	—	—	—	—

[a] Reference [38].
[b] Reference [33].
[c] Reference [9].
[d] Reference [11].
[e] Reference [12].
[f] Reference [39].
[g] Reference [3].
[h] Reference [4].
[i] Reference [5].
[j] Reference [40].
[k] Reference [6].
[l] Reference [35].

are smaller than the experimental data except in the case where the atomic energies are calculated within the DFT approach with an exchange–correlation potential parametrized according to the local approximation (LP). As expected, the agreement with experiment is satisfactory for MgO and CaO with the non-local DFT approach (BL) and especially with the '*a posteriori*' correlation correction to the HF energies described by the Becke GGA potential. However, the quality of the agreement decreases with the increase of the cation size, reaching 15% in the BaO case within this last approach.

3.2. The bulk modulus and $B_1 \rightleftharpoons B_2$ transition parameters

The theoretical curves $E(V)$ calculated at the HF, LP, BL, PBE and PP levels and fitted to the Murnaghan equation of state give the equilibrium unit-cell volume V_0, and the bulk modulus B and its pressure derivative B'. These values are reported in table 4 for the B_1 and B_2 phases with the experimental data and the results of other calculations for comparison. Generally speaking, table 4 shows, as expected, that the changes of the B-values are in the opposite direction to those in the corresponding V_0-values. This is verified for either a given calculation method or a given compound and phase. In the sequence

Table 5. Transition parameters obtained at the Hartree–Fock and density functional theory levels. P, V_{tr} and $\Delta V_{tr}/V_0$ (%) are the transition pressure (GPa), the transition volume (Å^3) and the volume collapse, where V_0 is the equilibrium volume of the B_1 phase. The symbols LP, BL, PBE and PP are defined in table 2.

			P	$V_{tr}(B_1)$	$V_{tr}(B_2)$	$\Delta V_{tr}/V_0$ (%)
MgO	This work	HF	711.6	9.0	8.7	3.6
		LP	511.8	9.3	8.9	4.9
		BL	478.1	9.8	9.3	5.4
		PBE	428.4	10.0	9.4	5.5
		PP	417.8	10.1	9.5	6.2
	Experiment		>100[a,b]	—	—	—
	Other calculations		197.5[c]	—	—	5.4[c]
			251[d]	11.3[d]	10.8[d]	4.3[d]
			515.0[e]	—	—	4.7[e]
			1050.0[f]	—	—	4.8[f]
CaO (AE)	This work	HF	68.1	21.6	19.1	11.6
		LP	55.9	20.5	18.4	10.3
		BL	73.7	20.6	18.7	9.3
		PBE	63.4	21.0	18.8	10.6
		PP	66.3	20.6	18.8	8.7
	Experiment		60.0[g]	—	—	—
			65.0[h]	—	—	10[h]
			63.0[i]	20.7[i]	18.7[i]	10[i]
	Other calculations		55.7[c]	—	—	10.7[c]
			55[d]	20.9[d]	19.3[d]	7.9[d]
			54.2[e]	—	—	11.2[e]
			67.9[j]	—	—	—
			121[k]	—	—	—

B(LP) > B(HF) > B(GGA), it will be noted that the differences between the values obtained with the three GGA models (BL, PBE and PP) are very small and lead to a very satisfactory agreement with experiment. It can be observed that MgO constitutes an exception, because the experimental volume is very well reproduced at the HF level, corresponding thus to a very small correlation effect. The description of calcium either with an AE or an ECP basis set leads to very similar B- and V_0-values for the B_1 phase but to slightly different ones for the B_2 phase. This result shows that the ECP can be validly used to obtain satisfactory B- and V_0-values for these simple systems. However, the accuracy seems to be insufficient to give a true physical meaning to the fact that there is the slight difference between the B-values for the B_1 and B_2 phases of CaO, SrO and BaO whereas they are practically identical for MgO and CaO (AE).

The pressure of the transition between the B_1 and B_2 phases is deduced, as indicated in equation (2), from the equality of the enthalpy for the B_1 and B_2 phases. The values obtained in each calculation method are given in table 5 with the experimental data and the results of other calculations for comparison. Following Mehl *et al* who define the collapse volume as $\Delta V_{tr}/V_0(B_1)$ where $\Delta V_{tr} = V_{tr}(B_1) - V_{tr}(B_2)$, the values of this ratio were also obtained, and these are also reported in table 5. When compared to the available experimental data which are not very homogeneous except for CaO, the results given in

Table 5. (Continued)

			P	$V_{tr}(B_1)$	$V_{tr}(B_2)$	$\Delta V_{tr}/V_0$ (%)
CaO (PS)	This work	HF	75.1	21.2	19.0	10.4
		LP	65.1	20.6	18.4	10.7
		BL	80.2	20.8	18.8	9.7
		PBE	87.8	19.5	18.1	7.2
		PP	73.3	20.8	18.7	9.9
SrO	This work	HF	42.3	27.9	24.6	11.8
		LP	29.2	27.4	24.0	12.3
	Experiment		36[l]	27.5[l]	24.1[l]	13.0[l]
	Other calculations		33.5[m]	—	—	12.8[m]
			31.7[c]	—	—	11.4[c]
			36[d]	26.3[d]	24.2[d]	7.9[d]
			35[n]	—	—	10[n]
BaO	This work	HF	27.3	36.6	32.1	12.3
		LP	17.4	36.0	31.2	13.3
	Experiment		9[o]	—	—	—
			14.5[p]	—	—	—
	Other calculation		21[d]	34.0[d]	31.2[d]	8.3[d]

[a] Reference [1].
[b] Reference [2].
[c] Reference [9].
[d] Reference [10].
[e] Reference [11].
[f] Reference [12].
[g] Reference [3].
[h] Reference [4].
[i] Reference [5].
[j] Reference [40].
[k] Reference [41].
[l] Reference [6].
[m] Reference [27].
[n] Reference [42].
[o] Reference [7].
[p] Reference [8].

table 5 indicate that our values of the transition parameters are on the whole in satisfactory agreement. However, our calculated values do not allow us to deduce the best-adapted calculation method in order to obtain the best transition parameters. The HF approximation gives higher values than the DFT approach in the local approximation (LP) except for the transition volumes. Two reasons can be invoked to account for the lack of accuracy of our theoretical results:

(i) the first one corresponds to the use of the B'-parameter, whose values deduced from the Murnaghan equation of state are determined with a moderate accuracy as indicated in table 4; and

(ii) the second one is attributable to the method used for determining the transition parameters: it requires an extrapolation of the $H(p)$ curves of the two phases towards

Table 6. The square roots of the atomic (M and O) spheropoles QR (au) and overlap populations (e^-) between the nearest (M–O) and second-nearest (O–O) neighbours evaluated at the HF level according to a Mulliken partition of the charge density. The M–O and O–O distances (Å) are given in italics at $p = 0$. The overlap populations at the transition pressure are given in parentheses.

B_1			B_2		
Mg		2.3	2.5		Mg
O		4.3	4.1		O
Mg–O	*2.10*	0.001	0.016	*2.25*	Mg–O
		(−)	(−)		
O–O	*2.97*	−0.019	−0.116	*2.60*	O–O
		(−)	(−)		
Ca		3.9	3.9		Ca
O		4.4	4.3		O
Ca–O	*2.43*	−0.037	−0.019	*2.55*	Ca–O
		(−0.100)	(−0.082)		
O–O	*3.44*	−0.005	−0.053	*2.95*	O–O
		(−0.019)	(−0.148)		
Sr		4.5	4.5		Sr
O		4.5	4.4		O
Sr–O	*2.61*	−0.057	−0.038	*2.72*	Sr–O
		(−0.112)	(−0.077)		
O–O	*3.69*	−0.001	−0.036	*3.14*	O–O
		(−0.008)	(−0.088)		
Ba		5.5	5.6		Ba
O		4.5	4.4		O
Ba–O	*2.83*	−0.063	−0.036	*2.94*	Ba–O
		(−0.121)	(−0.074)		
O–O	*3.99*	0.000	−0.008	*3.39*	O–O
		(−0.002)	(−0.019)		

pressure values rather distant from those corresponding to the calculated $E(V)$ curves, especially for MgO.

Finally, the changes of the transition pressure within the series of alkaline-earth oxides can be related particularly well to the size of the ions and to the populations of the bond between the nearest (M–O) and second-nearest (O–O, M–M) neighbours which lead to the crystal compressibility. These two structural features are determined from a Mulliken scheme for the partition of the charge density, which shows also the fully ionic character of each compound in both phases. The size of the ions is evaluated from the square root QR of the atomic spheropole and reported in table 6, with the bond populations only at the HF level for reasons of clarity.

The spheropole QR^2 is defined according to the following equation:

$$\int \rho_A |r_A|^2 \, \mathrm{d}r \tag{3}$$

where ρ_A (r) is the atomic electron charge density and $|r_A|^2 \approx |r - s_A|^2$ is an operator which is function of the position s_A at which the atom A is located. All of the methods of calculation lead to very similar results and the largest differences are observed between the HF and LP results. The LP atomic spheropoles are slightly larger than the corresponding

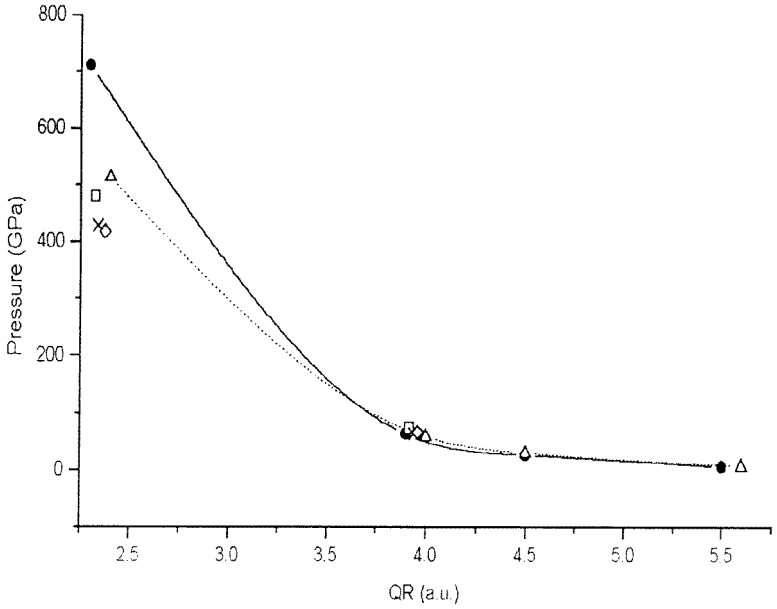

Figure 1. The transition pressure (GPa) versus the square root of the M spheropoles QR (au) calculated according to a Mulliken partition of the charge density. The symbols •, △, □, × and ◇ correspond to the HF, LP, BL, PBE and PP calculations, respectively. The full and dotted lines are the best fits for the HF and LP results.

HF ones. For the cation, the difference changes from 6% in MgO (B_2) to 0% (SrO and BaO) whereas it is practically the same (2%) for the oxygen. This result, when compared to the decrease of the lattice parameter calculated with the LP method compared to that calculated with the HF method shows that a part of the electron correlation introduced in the LP approach enlarges the overlapping of the electron clouds more than the size of the ions. The size of a given alkaline-earth cation is the same in phases B_1 and B_2 except that of Mg^{2+} which is expanded in phase B_2 by about 10% with respect to that in phase B_1. The O^{2-} size is nearly constant for both phases of the four compounds: it seems however slightly smaller in phase B_2 than in phase B_1 especially for MgO and CaO. The transition pressure which is dependent on both B_1 and B_2 structures can be related only to the B_1 (or B_2) geometrical structure in view of the previous remarks. The best fit between the alkaline-earth QR values (table 6) and its corresponding transition pressure can be described according to a relationship which has the form $P = ae^{b(\mathrm{QR})}$, to take into account particularly the MgO transition pressure, which however is not accurate (figure 1). The values of the a- and b-parameters are $a = 22.9 \times 10^3$, $b = -1.51$ and $a = 13.4 \times 10^3$, $b = -1.36$ for the HF and LP results, respectively.

All of the bond populations are negative except the Mg–O one especially for phase B_2 and those corresponding to the M^{2+}–M^{2+} second-nearest neighbours, which are always null. This indicates an antibonding character of the interactions between the O^{2-}–O^{2-} second-nearest neighbours and the M^{2+}–O^{2-} first-nearest neighbours when M ≡ Ca, Sr and Ba. As expected, the antibonding character corresponding to the O^{2-}–O^{2-} interaction is enlarged when its distance is decreased, i.e. from BaO to MgO in phases B_1 and B_2 and from phase B_1 to phase B_2 in a given compound and, of course, from $p = 0$ to the transition pressure. The cation–oxygen (M^{2+}–O^{2-}) interaction leads generally to a negative bond

population whose strength increases with the M^{2+}–O^{2-} distance. This bond population is more negative in phase B_1 than in phase B_2 but its changes versus the M^{2+}–O^{2-} distance are similar for the two phases. Finally, the values of the transition pressure seem therefore to be determined more by the repulsive O^{2-}–O^{2-} interaction, especially in phase B_2, than by the same interactions in phase B_1 or by the M^{2+}–O^{2-} interactions in both phases.

4. Conclusions

A series of simple closed-shell compounds with high-symmetry structures, allowing us to achieve high numerical accuracy, has been chosen to make a valid comparison of the trend of the HF and different DF models to reproduce better the experimental geometries, binding energy, bulk modulus and $B_1 \rightleftharpoons B_2$ transition pressures and volumes. In this series, the contribution of the electronic correlation to the calculated properties increases with the cation size, and the efficiency of the correction to the HF charge density as a result of using a DF model can be appreciated more easily when the cation belongs to a higher row of the periodic table. Generally speaking, the DF method using a non-local correction of $\rho(\boldsymbol{r})$ seems to be of better quality than that using an exchange–correlation potential parametrized according to a local model. That is particularly true for the binding energy and above all for the determination of the bulk modulus. However, the correction of the HF lattice parameter as a result of using the DF non-local models is practically null whereas that obtained as a result of using the LDA is large and makes the calculated lattice parameter smaller than the experimental one. In the light of these results, it is difficult to deduce the best 'non-local' DFT-corrected scheme among the three (BL, PBE and PP) investigated in this work, but it seems that the non-local exchange–correlation potential of Becke and of Lee, Yang and Parr (BL) is less well adapted for calculating the lattice parameters.

For the determination of the phase transition parameters, we must recall that the accuracy of their values depends substantially on the derivative B' which, as a general rule, is not very accurate and on the degree of extrapolation of the enthalpy curves. These factors explain why the phase transition parameters cannot be obtained, as a general rule, with a great accuracy. This is verified in our work, where the calculated transition pressures are fluctuating and the 'non-local' DF values are actually similar to the HF ones but those calculated using the LDA are always smaller. Before concluding with a generalization of these results, it would be interesting to examine other simple systems containing transition metals which will be described with the unrestricted Hartree–Fock method and the same DF methods.

References

[1] Carter W J, Marsh S P, Fritz J N and McQueen R G 1971 *NBS Special Publication 326* p 147
[2] Mao H K and Bell P 1979 *J. Geophys. Res.* **84** 4533
[3] Richet P, Mao H K and Bell P M 1986 *J. Geophys. Res.* **93** 15 279
[4] Jeanloz R, Ahrens T J, Mao H K and Bell P M 1979 *Science* **206** 829
[5] Mammone J F, Mao H K and Bell P M 1981 *Geophys. Res. Lett.* **8** 140
[6] Sato Y and Jeanloz R 1981 *J. Geophys. Res.* **86** 11
Sato Y and Jeanloz R 1981 *J. Geophys. Res.* **86** 773
[7] Liu L G and Basset W A 1972 *J. Geophys. Res.* **77** 4934
[8] Liu L G 1971 *J. Appl. Phys.* **42** 3702
[9] Kalpana G, Palanivel B and Rajagopalan M 1995 *Phys. Rev.* B **52** 4
[10] Mehl M J, Hemley R J and Boyer L L 1986 *Phys. Rev.* B **33** 8685
[11] Mehl M J, Cohen R E and Krakauer H 1988 *J. Geophys. Res.* **93** 8009
[12] Chang K J and Cohen L 1984 *Phys. Rev.* B **30** 4774

[13] Murnaghan F D 1944 *Proc. Natl Acad. Sci. USA* **30** 244
[14] Dovesi R, Saunders V R, Roetti C, Causà M, Harrison N M, Orlando R and Aprà E 1996 *CRYSTAL95 User's Manual* University of Torino
[15] Pisani C, Dovesi R and Roetti C 1988 *Hartree–Fock ab initio Treatment of Crystalline Systems (Springer Lecture Notes in Chemistry 48)* (Berlin: Springer)
[16] Saunders V R, Freyria-Fava C, Dovesi R, Salasco L and Roetti C 1992 *Mol. Phys.* **77** 629
[17] Dirac P A M 1930 *Proc. Cambridge Phil. Soc.* **26** 376
[18] Perdew J P and Zunger A 1981 *Phys. Rev.* B **23** 5048
[19] Becke A D 1988 *Phys. Rev.* A **38** 3098
[20] Lee C, Yang W and Parr R G 1988 *Phys. Rev.* B **37** 785
[21] Perdew J P, Burke K and Ernzerhof M 1996 *Phys. Rev.* **77** 3865
[22] Perdew J P and Wang Y 1986 *Phys. Rev.* B **33** 8800
Perdew J P and Wang Y 1989 *Phys. Rev.* B **40** 3399
[23] Hay P J and Wadt W R 1985 *J. Chem. Phys.* **82** 270
Hay P J and Wadt W R 1985 *J. Chem. Phys.* **82** 284
Hay P J and Wadt W R 1985 *J. Chem. Phys.* **82** 299
[24] Catti M, Valerio G, Dovesi R and Causà M 1994 *Phys. Rev.* B **49** 14 179
[25] Causà M, Dovesi R, Pisani C and Roetti C 1986 *Phys. Rev.* B **33** 1308
Dovesi R, Roetti C, Freyria-Fava C, Aprà E, Saunders V R and Harrison N M 1992 *Phil. Trans. R. Soc.* A **34** 203
[26] Catti M, Dovesi R, Pavese A and Saunders V R 1991 *J. Phys.: Condens. Matter* **3** 4151
[27] Zupan A, Petek I, Causà M and Dovesi R 1993 *Phys. Rev.* B **48** 799
[28] Gordon R G and Kim Y S 1972 *J. Chem. Phys.* **56** 3122
[29] Kim Y S and Gordon R G 1974 *Phys. Rev.* B **9** 3548
[30] Cohen A J and Gordon R G 1975 *Phys. Rev.* B **12** 3228
[31] *GAUSSIAN94* 1994 Gaussian, Incorporated, Pittsburgh, PA
[32] Perdew J P and Wang Y 1992 *Phys. Rev.* B **45** 13 244
[33] Wyckoff R W G 1963 *Crystal Structure* (New York: Wiley)
[34] *Handbook of Mathematical Functions* 1972 ed M Abramowitz and I A Stegun (Washington, DC: US Government Printing Office) p 883
[35] Son P R and Bartels R A 1972 *J. Phys. Chem. Solids* **33** 819
[36] Michard F and Zarembowitch M A 1969 *C. R. Acad. Sci., Paris* B **30** 269
[37] *Janaf Thermodynamical Tables* 1985 *J. Phys. Chem. Ref. Data Suppl.* 1 **14**
[38] Anderson O L and Andreatch P Jr 1966 *J. Am. Ceram. Soc.* **49** 404
[39] Bukowinsky M S T 1985 *Geophys. Res. Lett.* **12** 536
[40] D'Arco Ph, Jolly L H and Silvi B 1992 *Phys. Earth Planet. Interiors* **72** 286
[41] Cohen A J and Gordon R G 1976 *Phys. Rev.* B **14** 4593
[42] Zhang H and Bukowinsky M S T 1991 *Phys. Rev.* B **44** 2495